

NATIONAL AERONAUTICS AND SPACE ADMINISTRATION

TECHNICAL REPORT

R-39

THE PHENOMENON OF CHANGE IN BUCKLE PATTERN IN ELASTIC STRUCTURES

By MANUEL STEIN

1959

TECHNICAL REPORT R-39

**THE PHENOMENON OF CHANGE IN BUCKLE PATTERN
IN ELASTIC STRUCTURES**

By MANUEL STEIN

**Langley Research Center
Langley Field, Va.**

TECHNICAL REPORT R-39

THE PHENOMENON OF CHANGE IN BUCKLE PATTERN IN ELASTIC STRUCTURES¹

By MANUEL STEIN

SUMMARY

By means of a rigorous analysis of a three-element column on a nonlinear elastic foundation, the phenomenon of change in buckle pattern is investigated. A discussion of how the present results may be applied to plates and other elastic structures is given.

INTRODUCTION

One of the phenomena which have been observed in the postbuckling behavior of various stiffened and unstiffened plates and shells is change in buckle pattern occurring when the buckle mode becomes unstable and the structure seeks a stable configuration. The point of instability of the original buckle mode has not been studied rigorously heretofore, and the mechanism of change has not been described. In order to analyze this phenomenon, a model was chosen which exhibits the important properties associated with a change in buckle pattern of plates and for which an exact solution could be obtained. The model chosen is a symmetric three-element column restrained by nonlinear springs which introduce the cubic nonlinear characteristics of plates and some other elastic structures. The present analysis includes a rigorous study of stability for this model in its various modes. The way in which the present results may be applied to other elastic structures is indicated.

SYMBOLS

l	length of each of three rigid rods
C	stiffness of torsional springs
K, K_1	stiffness of nonlinear extensional springs, force/length ³

P	total compressive load
w_1, w_2	deflection of joints in column (see fig. 1)
$w_{1,0}, w_{2,0}$	initial deflection of joints in column
$\xi = \frac{w_1 + w_2}{2}$	
$\eta = \frac{w_1 - w_2}{2}$	
Δ	total shortening
$\theta_1, \theta_2, \theta_3, \theta_4$	angles formed upon deflection of column (see fig. 1)

ANALYSIS

The model considered is a column consisting of three rigid rods connected by linear torsional springs and supported along the length by nonlinear extensional springs as shown in figure 1. The rods are of equal length, and the restoring force of each of the nonlinear springs is considered

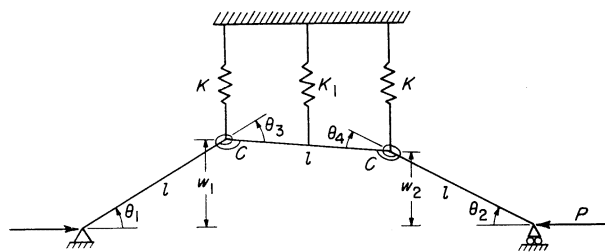


FIGURE 1.—Three-element column connected by linear torsional springs and laterally restrained by nonlinear extensional springs.

¹ The information presented herein was a part of a dissertation entitled "Postbuckling Behavior of Rectangular Plates" which was offered in partial fulfillment of the requirements for the degree of Doctor of Philosophy in Applied Mechanics, Virginia Polytechnic Institute, Blacksburg, Virginia, June 1958.

to be proportional to the cube of its displacement. The stability of this column is investigated for both the controlled-loading and controlled-shortening types of load application.

Since the stability is of interest, it is convenient to use an energy method of approach. The equilibrium configurations, that is, those configurations for which the potential energy is an extremum are found. These extremums are then investigated to see which of them are minimums (and hence imply stability) and which are not minimums (and hence imply instability). Solutions are presented in the form of load-shortening curves.

TOTAL POTENTIAL ENERGY

The potential energies of the elements of the system are summed to obtain the total potential energy. For the nonlinear springs, the force F in the spring is proportional to the cube of the displacement w of the spring; that is, $F=Kw^3$. The strain energy in a spring is related to the force and displacement as given in the expression $\int_0^w Fdw$. Thus, the potential (strain) energy of the nonlinear springs Π_1 is expressed by

$$\Pi_1 = \frac{K}{4}(w_1^4 + w_2^4) + \frac{K_1}{4}\left(\frac{w_1 + w_2}{2}\right)^4 \quad (1)$$

With the assumption that the deflections are small when compared with the length of the column, the angles are given in terms of the deflections by

$$\begin{aligned} \theta_1 &= \frac{w_1}{l} \\ \theta_2 &= \frac{w_2}{l} \\ \theta_3 &= \frac{2w_1 - w_2}{l} \\ \theta_4 &= \frac{2w_2 - w_1}{l} \end{aligned}$$

By making use of this assumption, the potential (strain) energy of the torsional springs Π_2 can be written as

$$\Pi_2 = \frac{C}{2} \left[\left(\frac{2w_1 - w_2}{l} \right)^2 + \left(\frac{2w_2 - w_1}{l} \right)^2 \right] \quad (2)$$

The shortening Δ of the column is

$$\Delta = l \{ 3 - [\cos \theta_1 + \cos \theta_2 + \cos (\theta_3 - \theta_1)] \}$$

or, with the assumption of small deflections,

$$\Delta = \frac{1}{2l} [w_1^2 + w_2^2 + (w_1 - w_2)^2] \quad (3)$$

The potential energy Π_3 of the load P is the negative product of load and shortening; therefore,

$$\Pi_3 = -\frac{P}{2l} [w_1^2 + w_2^2 + (w_1 - w_2)^2] \quad (4)$$

Before proceeding to use the equations just given for the energies, it is convenient to express w_1 and w_2 in terms of ξ and η according to

$$\xi = \frac{w_1 + w_2}{2}$$

$$\eta = \frac{w_1 - w_2}{2}$$

Note that when $\eta=0$ the deflections are symmetric, and when $\xi=0$ the deflections are antisymmetric. In terms of the new variables the energies expressed in equations (1), (2), and (4), respectively, become

$$\Pi_1 = \frac{K}{2} (\xi^4 + 6\xi^2\eta^2 + \eta^4) + \frac{K_1}{4} \xi^4 \quad (5)$$

$$\Pi_2 = \frac{C}{l^2} (\xi^2 + 9\eta^2) \quad (6)$$

$$\Pi_3 = -\frac{P}{l} (\xi^2 + 3\eta^2) \quad (7)$$

and equation (3) for the shortening becomes

$$\Delta = \frac{1}{l} (\xi^2 + 3\eta^2) \quad (8)$$

The total potential energy is

$$\Pi = \Pi_1 + \Pi_2 + \Pi_3$$

for controlled loading and

$$\Pi = \Pi_1 + \Pi_2$$

for controlled shortening. For controlled shortening the potential energy is equal to the strain energy of the system.

CONTROLLED LOADING

According to the minimum-potential-energy method, the variation of the total potential energy

of the system must vanish. For controlled loading, this requirement may be expressed by

$$\delta\Pi = \frac{\partial\Pi}{\partial\xi}\delta\xi + \frac{\partial\Pi}{\partial\eta}\delta\eta = 0$$

or, since the variations of ξ and η are perfectly arbitrary, by

$$\frac{\partial\Pi}{\partial\xi} = 0$$

$$\frac{\partial\Pi}{\partial\eta} = 0$$

Thus, the conditions for buckling are

$$\left. \begin{aligned} \xi \left[K(\xi^2 + 3\eta^2) + \frac{K_1}{2} \xi^2 + \frac{C}{l^2} - \frac{P}{l} \right] &= 0 \\ \eta \left[K(3\xi^2 + \eta^2) + 9\frac{C}{l^2} - 3\frac{P}{l} \right] &= 0 \end{aligned} \right\} \quad (9)$$

A possible solution for ξ and η is

$$\left. \begin{aligned} \eta &= 0 \\ \xi^2 &= \frac{2C}{l^2 K} \frac{\frac{Pl}{C} - 1}{2 + \frac{K_1}{K}} \end{aligned} \right\} \quad (10)$$

Another possible solution is

$$\left. \begin{aligned} \xi &= 0 \\ \eta^2 &= \frac{3C}{l^2 K} \left(\frac{Pl}{C} - 3 \right) \end{aligned} \right\} \quad (11)$$

There also exists a possible third solution where neither ξ nor η is zero:

$$\left. \begin{aligned} \xi^2 &= \frac{4C}{l^2 K} \frac{4\frac{Pl}{C} - 13}{16 - \frac{K_1}{K}} \\ \eta^2 &= \frac{3CK_1}{l^2 K^2} \frac{4\frac{K}{K_1} + 3 - \frac{Pl}{C}}{16 - \frac{K_1}{K}} \end{aligned} \right\} \quad (12)$$

This third solution gives deflections which are neither symmetric nor antisymmetric. Note that for the various possible solutions, limitations may be set down immediately on the ranges of loading

which may be considered. Real values of ξ and η and, therefore, of the deflections w_1 and w_2 will occur in the first solution only if $Pl/C > 1$, in the second if $Pl/C > 3$, and in the third if

either $\left(4\frac{K}{K_1} + 3\right) > \frac{Pl}{C} > \frac{13}{4}$ for $16K > K_1$ or $\frac{13}{4} > \frac{Pl}{C} > \left(4\frac{K}{K_1} + 3\right)$ for $K_1 > 16K$. In these ranges the three solutions represent equilibrium positions.

The shortening expressed in equation (8) can now be written for each of the three solutions. For $\eta = 0$,

$$\frac{Kl^3\Delta}{C} = 2 \frac{\frac{Pl}{C} - 1}{2 + \frac{K_1}{K}} \quad (13)$$

For $\xi = 0$,

$$\frac{Kl^3\Delta}{C} = 9 \left(\frac{Pl}{C} - 1 \right) \quad (14)$$

For both $\xi \neq 0$ and $\eta \neq 0$,

$$\frac{Kl^3\Delta}{C} = \frac{Pl}{C} - 1 - 2 \frac{K_1}{K} \frac{4\frac{Pl}{C} - 13}{16 - \frac{K_1}{K}} \quad (15)$$

These three equations are the load-shortening relations for the possible equilibrium positions (or modes) and are subject to the aforementioned limitations on P .

The stability of the column in each of the three modes is discussed next. For this column the second variation of the potential energy is

$$\delta^2\Pi = \frac{\partial^2\Pi}{\partial\xi^2} (\delta\xi)^2 + 2 \frac{\partial^2\Pi}{\partial\xi\partial\eta} (\delta\xi)(\delta\eta) + \frac{\partial^2\Pi}{\partial\eta^2} (\delta\eta)^2$$

For stability in a given equilibrium configuration, the second variation must be positive definite in the arbitrary $\delta\xi$ and $\delta\eta$ for this configuration. Thus, for stability, both of the coefficients of the squared terms must be positive, and the discriminant of the preceding quadratic form must be negative. If one or both of the coefficients of the squared terms are negative, or if the discriminant is positive, the equilibrium configuration is unstable.

The ranges of stability are as follows:

For $\eta = 0$,

$$1 < \frac{Pl}{C} < \left(4\frac{K}{K_1} + 3\right) \quad (16)$$

For $\xi=0$,

$$\frac{13}{4} < \frac{Pl}{C} \quad (17)$$

For both $\xi \neq 0$ and $\eta \neq 0$,

$$\left(4\frac{K}{K_1} + 3\right) < \frac{Pl}{C} < \frac{13}{4} \quad (18)$$

In all other ranges of equilibrium the column is unstable.

Load-shortening curves for the column subject to a controlled load are shown in figure 2 with the stable and unstable portions indicated. Each set of curves is composed of three straight lines. The line originating at $Pl/C=1$ (initial buckling load) represents the symmetric equilibrium configuration, the line originating at $Pl/C=3$ (unstable higher buckling load) represents the anti-symmetric equilibrium configuration, and a transition line which extends only between the other two lines represents the equilibrium configuration

which is neither symmetric nor antisymmetric. Similar load-shortening curves are described later for the column subject to controlled shortening and then both sets of curves are discussed.

CONTROLLED SHORTENING

For a loading of the type given by a controlled-shortening machine, the deflections w_1 and w_2 are related to each other in terms of the applied shortening Δ . In the variables ξ and η , this relationship is expressed by

$$l\Delta = \xi^2 + 3\eta^2$$

The potential energy for controlled shortening is the strain energy ($\Pi = \Pi_1 + \Pi_2$). The variable ξ may be eliminated from the strain energy to obtain

$$\begin{aligned} \Pi = \frac{K}{2} [(l\Delta - 3\eta^2)^2 + 6(l\Delta - 3\eta^2)\eta^2 + \eta^4] \\ + \frac{K_1}{4} (l\Delta - 3\eta^2)^2 + \frac{C}{l^2} (l\Delta + 6\eta^2) \end{aligned}$$

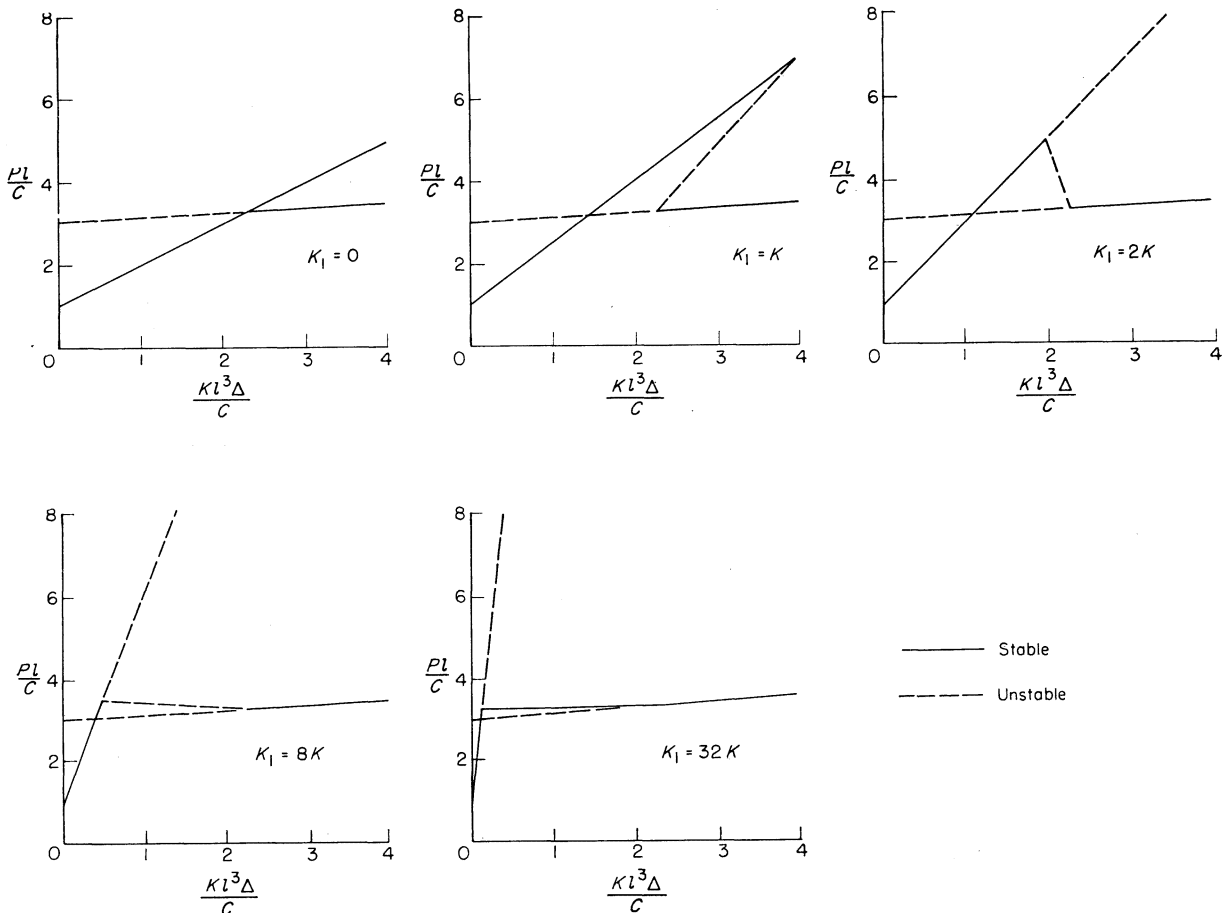


FIGURE 2.—Dimensionless load-shortening curves for the three-element column. Controlled loading.

According to the minimum-potential-energy method for this case

$$\delta\Pi = \frac{\partial\Pi}{\partial\eta} \delta\eta = 0$$

or, since the variation of η is arbitrary,

$$\frac{\partial\Pi}{\partial\eta} = \eta \left[-16K\eta^2 - 3K_1(l\Delta - 3\eta^2) + 12 \frac{C}{l^2} \right] = 0$$

Therefore, either

$$\left. \begin{array}{l} \eta = 0 \\ \xi^2 = l\Delta \end{array} \right\} \quad (19)$$

or

$$\left. \begin{array}{l} \eta^2 = 3 \frac{C}{l^2 K} \frac{4 - \frac{K_1 l^3 \Delta}{C}}{16 - 9 \frac{K_1}{K}} \\ \xi^2 = l\Delta - 9 \frac{C}{l^2 K} \frac{4 - \frac{K_1 l^3 \Delta}{C}}{16 - 9 \frac{K_1}{K}} \end{array} \right\} \quad (20)$$

Alternatively, by substituting for η instead of ξ in the equation expressing potential energy and then varying the potential energy with respect to ξ instead of η , the following additional result is obtained:

$$\left. \begin{array}{l} \xi = 0 \\ \eta^2 = \frac{l\Delta}{3} \end{array} \right\} \quad (21)$$

Note that the three sets of results given by equations (19), (20), and (21) can be classified, respectively, by $\eta=0$, by both $\xi \neq 0$ and $\eta \neq 0$, and by $\xi=0$.

In order to plot load-shortening curves, as was done for controlled loading, use is made of the fact that the derivative of the equation for strain energy with respect to the shortening is equal to the reaction compressive load P . First substitute for ξ and η in the equation for strain energy for each of the three cases. Then differentiation of the equation for strain energy with respect to Δ leads to expressions for P which are identical to those obtained for controlled loading. Thus, the equilibrium configurations are the same for both types of loads, as might be expected. The stability of these equilibrium configurations, however, can be different.

The second variation of the equation for potential energy from which ξ has been eliminated is

$$\delta^2\Pi = \frac{\partial^2\Pi}{\partial\eta^2} (\delta\eta)^2$$

Similarly, the second variation of the equation for potential energy from which η has been eliminated is

$$\delta^2\Pi = \frac{\partial^2\Pi}{\partial\xi^2} (\delta\xi)^2$$

Since, for stability, the second variation must be positive, both $\frac{\partial^2\Pi}{\partial\eta^2}$ and $\frac{\partial^2\Pi}{\partial\xi^2}$ must be positive for the various equilibrium solutions to be stable. Use of these conditions leads to the following ranges of stability:

For $\eta=0$,

$$l\Delta < \frac{4C}{l^2 K_1} \quad (22)$$

For $\xi=0$,

$$l\Delta > \frac{9C}{4l^2 K} \quad (23)$$

For both $\xi \neq 0$ and $\eta \neq 0$,

$$\frac{9C}{4l^2 K} > l\Delta > \frac{4C}{l^2 K_1} \quad (24)$$

In all other ranges of equilibrium the column is unstable.

Load-shortening curves for both the stable and unstable configurations for the column subject to a controlled shortening are shown in figure 3. These curves are identical to those obtained for controlled loading in figure 2, except that in some ranges the curves of figure 3 represent stable configurations, whereas, in figure 2 they represent unstable configurations.

RESULTS AND DISCUSSION

The results shown in figures 2 and 3 have some very interesting features. For a better understanding of these features, consider the schematic diagram in figure 4 of the load-shortening curves of a column corresponding roughly to the results presented in figures 2 and 3 for $K_1=2K$. When subject to controlled shortening (fig. 4(a)), the column first buckles (at A) into a symmetric buckle pattern (AB; $\eta=0$). As the shortening increases, the load supported by the column increases

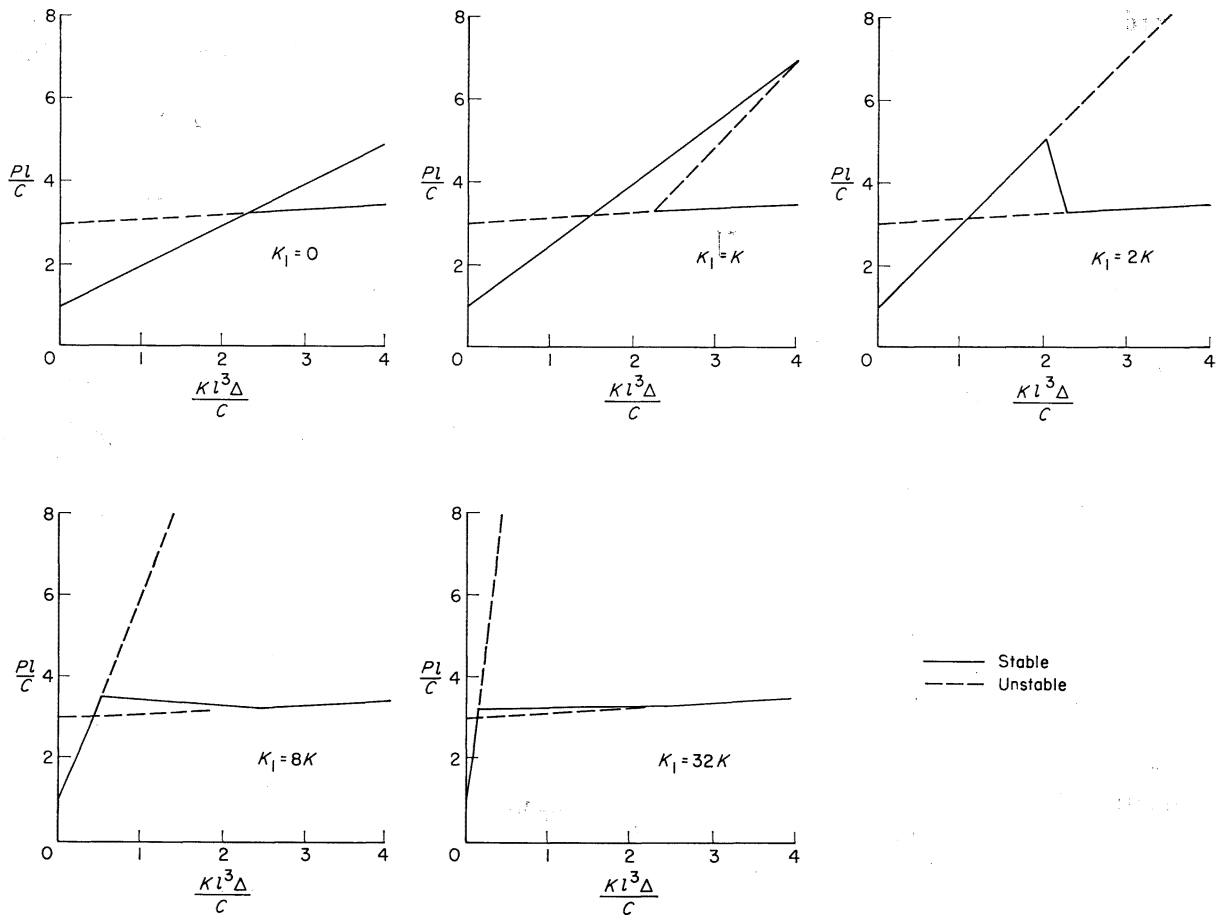


FIGURE 3.—Dimensionless load-shortening curves for the three-element column. Controlled shortening.

up to the secondary buckling load (B) which occurs at the intersection of the transition curve (BC; both $\xi \neq 0$ and $\eta \neq 0$) and the curve for symmetric buckling. The transition curve provides a continuous stable equilibrium path from the curve for symmetric buckling to the curve for antisymmetric buckling (CD; $\xi = 0$). Thus, as the shortening is increased beyond the secondary buckling load, the load falls and then begins to rise again. If the shortening is now decreased (for example, at D), the path is retraced as is indicated in figure 4(a) (DEFG).

The load-shortening curve for the same column subject to a controlled load is shown schematically in figure 4(b). For this case the transition curve (IL) does not represent a stable equilibrium configuration. As the load is increased beyond that for secondary buckling (I), the column, in seeking a stable equilibrium configuration, changes buckle pattern abruptly from the symmetric (HI) to the

antisymmetric (JK) form. Since the load is controlled, the change in buckle pattern occurs at a constant load (IJ). (For a case of controlled shortening when there are no continuous stable paths available, the jump is at constant shortening.) Upon unloading (at K, for instance), the antisymmetric pattern provides a stable path only for loads greater than the intersection of the curve for antisymmetric buckling with the transition curve (that is, from K to L). When this load (at L) is reached, there is again an abrupt change in buckle pattern at constant load (LM) back into the symmetric form. The area enclosed in the loop so formed, as shown in figure 4(b) (IJLM), is a measure of the energy expended in the abrupt changes. Here the system behaves nonconservatively, while the system considered in figure 4(a) behaves conservatively.

Of the results presented in figures 2 and 3, continuous stable equilibrium paths in the transition

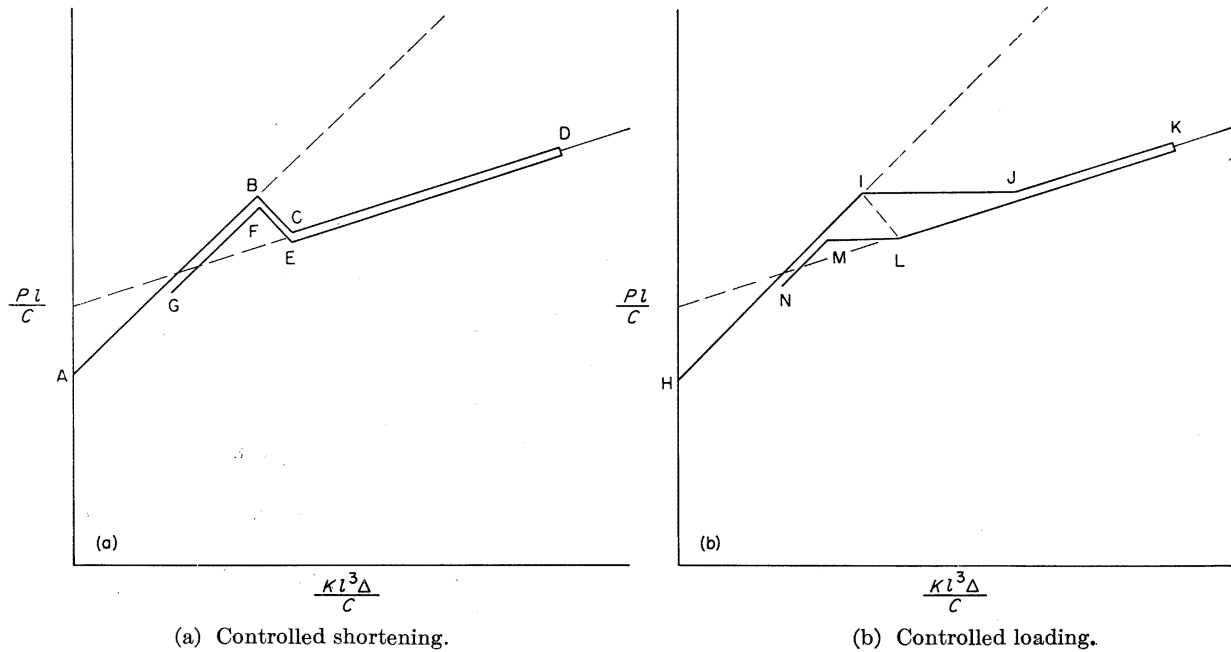


FIGURE 4.—Schematic diagrams of loading and unloading of a particular column which has a stable transition for controlled shortening and unstable transition for controlled loading.

from the symmetric to the antisymmetric buckle configuration occur for both controlled loading and controlled shortening only for high values of K_1 . For low values of K_1 the stability of the equilibrium curves indicates that abrupt changes will occur for both kinds of loadings. For intermediate values of K_1 , continuous stable equilibrium paths are available when the column is subject to controlled shortening but are not available when the column is subject to a controlled load, as just shown in the discussion of figure 4.

The results shown in figures 2 and 3 indicate that the load-shortening curves determining equilibrium and the point of secondary buckling are independent of the method of loading but that some segments of the load-shortening curves are stable or unstable according to the method of loading. Stability occurs as one might expect intuitively. For example, for a controlled load, if the transition path from the curve for symmetric buckling to that for antisymmetric buckling indicates an increasing load, then the transition path is stable; otherwise, the transition path is unstable.

Note that the access from the symmetric to the antisymmetric configuration is available only after secondary buckling, and secondary buckling always occurs for loads and shortenings greater than

those given by the intersection of the load-shortening curves for the symmetric and antisymmetric equilibrium configurations. Thus, intersections of load-shortening curves for the various equilibrium configurations indicate impending (but not necessarily imminent) changes in buckle patterns. (This condition existed for the model analyzed for every case except for the trivial case of $K_1=0$ where the changes in buckle patterns occurred at infinite load.)

The system under consideration, of course, is a conservative one, and, so long as equilibrium paths are followed, the system behaves conservatively. Therefore, the strain energy is equal to the area under the load-shortening curve if equilibrium paths (stable or unstable) are followed. Since the strain energy is independent of the path, so is the area under the load-shortening curve independent of the equilibrium paths. As a consequence, it can be seen in figures 2 and 3 that the area within the triangle to the right of the intersection of the load-shortening curves for the symmetric and antisymmetric equilibrium configurations is equal to the area within the triangle to the left of this intersection.

In order that the change in buckle pattern during loading may be better visualized, the deflections have been plotted in figure 5 for one of the

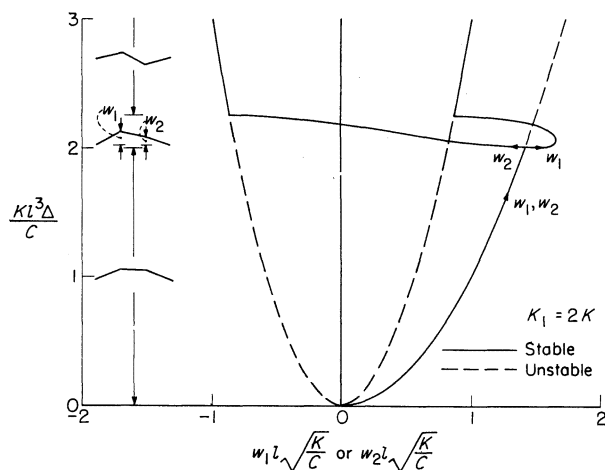


FIGURE 5.—Dimensionless equilibrium deflections of a three-element column. Controlled shortening.

columns which has a continuous loading path for controlled shortening as indicated by its load-shortening curve in figure 3. At the point shortening begins, the column buckles into a symmetric configuration ($w_1 = w_2$) as indicated by the solid curve starting from the origin in figure 5. With increases in shortening, the deflections increase until the shortening required for secondary buckling is reached. At this point and with an increase in shortening a stable transition configuration is formed which is neither symmetric nor antisymmetric ($w_1 \neq \pm w_2$). Continuing to increase the shortening in this transition range leads to an antisymmetric configuration ($w_1 = -w_2$), and still

more increases lead to larger deflections in the antisymmetric configuration. The arrows along the curves in figure 5 indicate the directions the deflections would take upon loading. The deflections would take the opposite directions for unloading.

The equations of the present study may be extended to include the effects of initial deflection in a straightforward manner. Some typical results of this extension are presented in figure 6. In addition to the load-shortening curve for a column with zero initial deflection, curves are shown for a column with symmetric initial deflection ($w_{1,o} = w_{2,o} = 0.1 \sqrt{\frac{C}{KL^2}}$) and for a column with asymmetric initial deflection ($w_{1,o} = 0.2 \sqrt{\frac{C}{KL^2}}$ and $w_{2,o} = 0$). These results show that a column

with initial deflections can have either a higher or a lower secondary buckling load than an initially straight column. As might be expected, this secondary buckling load occurs at a larger shortening for a column with initial deflections than for an initially straight column. The ranges of stable equilibrium for the column with initial deflections follow the same general pattern as for the initially straight column.

No curve is shown for a purely antisymmetric initial deflection since no change in buckle pattern

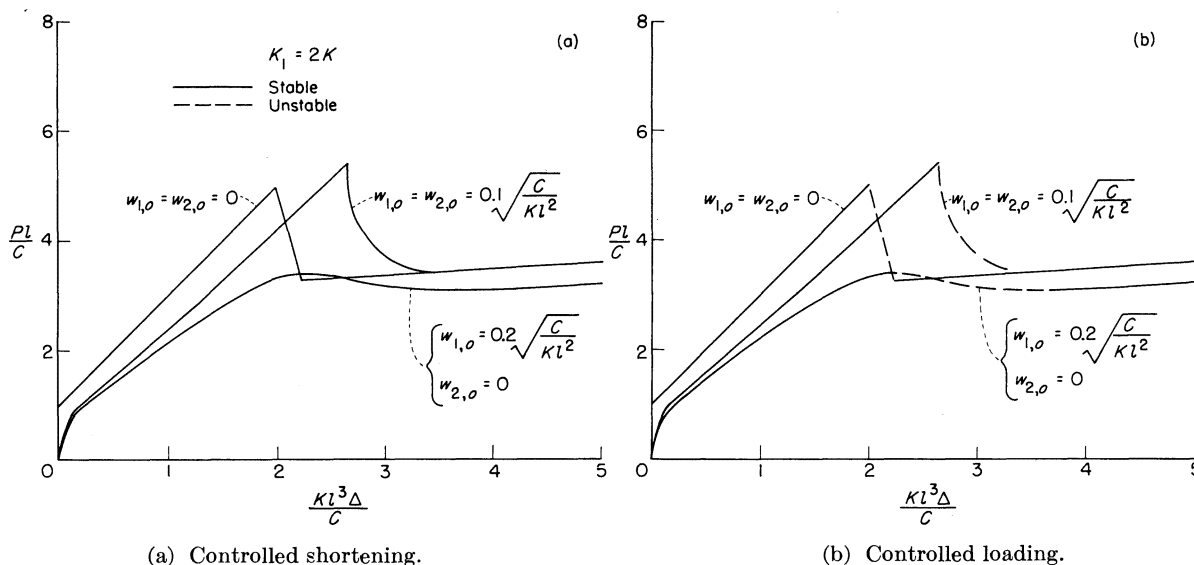


FIGURE 6.—Dimensionless load-shortening curves showing the effects of initial deflections $w_{1,o}$ and $w_{2,o}$ for a three-element column.

occurs. The column immediately assumes the antisymmetric configuration and remains in that configuration.

EXTENSION TO OTHER PROBLEMS

The results just obtained for the initially straight three-element column on a nonlinear elastic foundation indicate that loading beyond the load corresponding to the intersection of curves for the various equilibrium configurations of an initially perfect elastic structure ultimately brings about a change in the buckle pattern. The load (or shortening) at which a change in buckle pattern takes place is known once all the equilibrium paths of loading have been determined from the basic equations. In determining these paths it should be remembered that, for a conservative system, these (continuous) equilibrium paths will lead to the same strain energy regardless of the path of loading. In order to determine the stability of an equilibrium position for the three-element column subject to a certain type of loading, it was necessary to examine the second variation of the total potential energy. It is supposed that such a procedure would also be necessary for other problems.

For a system having abrupt changes in buckle patterns, hysteresis-type loops in the load-shortening curves can be calculated where the area of the loop will indicate the energy losses.

The behavior of the three-element column is directly analogous to the behavior of flat plates in the postbuckling range as specified by the Von Kármán large-deflection theory for plates, since the nonlinear restraint of the springs on the column is much like the nonlinear restraint of stretching of the plate middle surface (see ref. 1). Some of the load-shortening curves of the present analysis for the three-element column resemble the familiar load-shortening curves for a thin-walled cylinder in axial compression if the prebuckling configuration for the cylinder is likened to the first

(symmetric) equilibrium configuration for the column. Thus, in the question of the mechanism of change in buckle pattern, the present analysis affirms the principle that the initial equilibrium configuration is maintained until it becomes unstable, at which point the structure seeks another stable equilibrium configuration. This principle contrasts with the energy principle introduced in references 2 and 3.

CONCLUDING REMARKS

The analysis of a simple model has been presented which indicates the action of change in buckle pattern for two types of loading. The results indicate that, for initially perfect specimens, intersections between curves for the various equilibrium configurations lead to changes in the buckle patterns. The load at which a change in a buckle pattern occurs is shown to be independent of the type of loading, but the manner of change does depend on the type of loading. The change can be continuous or discontinuous, depending on the structure and on the type of loading. For the case where the change was continuous, for the model analyzed, a stable transition equilibrium configuration which was neither symmetric nor antisymmetric provided the path of change from the symmetric to the antisymmetric equilibrium configuration.

LANGLEY RESEARCH CENTER,
NATIONAL AERONAUTICS AND SPACE ADMINISTRATION,
LANGLEY FIELD, VA., *January 30, 1959.*

REFERENCES

1. Stein, Manuel: Loads and Deformations of Buckled Rectangular Plates. NASA TR R-40, 1959.
2. Tsien, H. S.: Buckling of a Column With Non-Linear Lateral Supports. *Jour. Aero. Sci.*, vol. 9, no. 4, Feb. 1942, pp. 119-132.
3. Tsien, Hsue-Shen: A Theory for the Buckling of Thin Shells. *Jour. Aero. Sci.*, vol. 9, no. 10, Aug. 1942, pp. 373-384.